Departmental Papers (CBE)

Department of Chemical & Biomolecular Engineering

August 2003

The Effect of Oxide Dopants in Ceria on *n*-Butane Oxidation

S. Zhao
University of Pennsylvania

Raymond J. Gorte
University of Pennsylvania, gorte@seas.upenn.edu

Recommended Citation

Zhao, S., & Gorte, R. J. (2003). The Effect of Oxide Dopants in Ceria on *n*-Butane Oxidation. Retrieved from http://repository.upenn.edu/cbe_papers/55

Postprint version. Published in *Applied Catalysis A: General*, Volume 248, Issues 1-2, 8 August 2003, pages 9-18.
Publisher URL: http://dx.doi.org/10.1016/S0926-860X(03)00102-9

The Effect of Oxide Dopants in Ceria on *n*-Butane Oxidation

Abstract

Solid solutions of CeO_2 with Yb_2O_3, Y_2O_3, Sm_2O_3, Gd_2O_3, La_2O_3, Nb_2O_5, Ta_2O_5, and Pr_6O_{11} were prepared by sol-gel methods. All of the samples exhibited a single, cubic phase in x-ray diffraction and the lattice parameters were consistent with formation of the solid solutions. Surprisingly, all of the mixed oxides exhibited a much lower catalytic activity for *n*-butane oxidation than that of pure CeO_2 at 650 K, with $Sm_{0.2}Ce_{0.8}O_{1.9}$, $Gd_{0.2}Ce_{0.8}O_{1.9}$, $La_{0.2}Ce_{0.8}O_{1.9}$, $Nb_{0.1}Ce_{0.9}O_{2.05}$, and $Ta_{0.1}Ce_{0.9}O_{2.05}$ showing rates less than 10^{-2} that of pure ceria. Lower dopant levels with Sm^{+3} and Gd^{+3} affected the rates proportionately less. The implications of these results for use of ceria as an oxidation catalyst are discussed.

Keywords

ceria, doped ceria, butane oxidation, ionic conductivity, samaria, gadolinia, lanthana, niobia, praeseodymia, tantala

Comments

Postprint version. Published in *Applied Catalysis A: General*, Volume 248, Issues 1-2, 8 August 2003, pages 9-18.
Publisher URL: http://dx.doi.org/10.1016/S0926-860X(03)00102-9

The Effect of Oxide Dopants in Ceria on n-Butane Oxidation

S. Zhao and R. J. Gorte
Department of Chemical Engineering
University of Pennsylvania,
Philadelphia, PA 19104

Abstract

Solid solutions of CeO_2 with Yb_2O_3, Y_2O_3, Sm_2O_3, Gd_2O_3, La_2O_3, Nb_2O_5, Ta_2O_5, and Pr_6O_{11} were prepared by sol-gel methods. All of the samples exhibited a single, cubic phase in x-ray diffraction and the lattice parameters were consistent with formation of the solid solutions. Surprisingly, all of the mixed oxides exhibited a much lower catalytic activity for n-butane oxidation than that of pure CeO_2 at 650 K, with $Sm_{0.2}Ce_{0.8}O_{1.9}$, $Gd_{0.2}Ce_{0.8}O_{1.9}$, $La_{0.2}Ce_{0.8}O_{1.9}$, $Nb_{0.1}Ce_{0.9}O_{2.05}$, and $Ta_{0.1}Ce_{0.9}O_{2.05}$ showing rates less than 10^{-2} that of pure ceria. Lower dopant levels with Sm^{+3} and Gd^{+3} affected the rates proportionately less. The implications of these results for use of ceria as an oxidation catalyst are discussed.

Key Words: ceria; doped ceria; butane oxidation; ionic conductivity; samaria; gadolinia; lanthana; niobia; praeseodymia; tantala.

Introduction

Among base-metal oxides, ceria is one of the better hydrocarbon-oxidation catalysts [1, 2]. For example, ceria has been reported to be the most active of the rare-earth oxides for total oxidation of butane by a considerable margin [1,3,4]. While ceria-based oxidation catalysts are normally coupled with a precious metal, alumina-supported ceria shows sufficient activity to be used for the oxidation of unburned hydrocarbons in diesel exhausts, even without the addition of precious metals [5,6].

One of the most intriguing aspects of ceria catalysis is that its properties depend strongly on pretreatment conditions and on mixing with other oxides. For example, when precious metals are supported on ceria films that have been calcined at temperatures below 1073 K, the catalytic properties of the material are consistent with facile transfer of oxygen from ceria to the metal [7-9]. The oxidation of Pd films by an underlying ceria-zirconia support was also observed spectroscopically to occur at moderate temperatures [10]. However, when ceria is calcined to higher temperatures, it becomes more difficult to reduce, resulting in a significant decrease in the activity of ceria-supported metals [11-13]. Consistent with this, CeO_2 single crystals, which by definition have been heated to high temperatures in their preparation, are difficult to reduce except by very harsh treatments such as ion sputtering [14,15]. Deactivation of the oxygen storage capacity of ceria by high temperatures in automotive applications is well known, and it is necessary to stabilize the reducibility of ceria for that application by mixing it with zirconia [16].

It is not really understood why the properties of ceria are so variable, but a number of ideas have been proposed. For pure ceria, crystallite size is often proposed for explaining the dependence of pretreatment conditions; however, in our laboratory, the deactivation of ceria occurred at temperatures significantly below that at which crystallite size increased [8]. Furthermore, crystallite size for ceria did not have any effect on the specific rates observed on ceria-supported Pd catalysts for the water-gas-shift reaction [17]. The increased reducibility of ceria-zirconia mixtures is usually explained by formation of solid solutions [18]. Again, others have reported that the most active form of ceria-zirconia is not a true solid solution [19]; and thick films of ceria on zirconia substrates were shown to be highly reducible, even when no solid solution had been formed [20-22]. Another possibility is that the facile reduction of ceria is associated with defect sites. Support for this mechanism has come from a correlation between the reducibility of ceria and ceria-zirconia mixtures and the defect density in ceria measured by neutron scattering measurements [22].

Because both the catalytic properties and the ionic conductivity of ceria are due to the ability of Ce to be in either the +3 or +4 oxidation states, it is common to look to the literature on solid electrolytes for ideas on enhancing catalytic activity. Doping, particularly with Sm^{+3} or Gd^{+3}, increases the ionic conductivity significantly by introducing oxygen vacancies [23]. The maximum ionic conductivity for +3 ions appears to be at a ratio of 4 (e.g. $Ce_{0.8}Gd_{0.2}O_x$) [23]. The ionic conductivity of ceria is also enhanced by doping with other rare earth oxides, and the conductivity of the doped ceria depends on the ionic radius of the doping ion [23] and the effect that this radius has on distorting the lattice [24]. It has been suggested that the anion vacancies produced by the introduction of +3 ions into ceria may enhance catalytic activity [25].

Doping with others ions could lead to enhanced activity for different reasons. For +5 ions, like Nb, one might be able to introduce extra oxygen anions that would be more easily removed [26]. Praseodymia is of interest because Pr_6O_{11} is much more easily reduced than CeO_2, but the catalytic activity of praseodymia seems to be limited by the difficulty in re-oxidizing Pr_2O_3 [27]. If one could use ceria to re-oxidize praseodymia, one might be able to take advantage of the higher reducibility of praseodymia. Indeed, there are indications that materials with enhanced properties can be prepared [25,28].

In this paper, we set out to investigate the effect of various dopants on the oxidation activity for n-butane. Our interest in the use of n-butane oxidation comes from the fact that n-butane is an ideal fuel for direct-oxidation, solid-oxide fuel cells [29,30]. Ceria is an important component in these fuel cells, at least in part due to its high activity for total oxidation of the hydrocarbon [4]. What we will show here is that doping ceria decreased its activity for all of the dopants we investigated. While other catalyst preparation conditions may lead to different results, our data clearly demonstrate that one cannot assume that dopants will increase activity in ceria.

Experimental

Catalyst Preparation

A complete list of the catalysts used in this study is given in Table 1. The properties of the pure ceria powder, prepared by decomposing $Ce(NO_3)_3{\cdot}6H_2O$ (Alfa Aesar, 99.5% purity) in air at 873 K, have been described in previous papers [31, 32]. The pure lanthana powder was also formed by calcination of $La(NO_3)_3{\cdot}6H_2O$ in air at 873K. Most of the doped-ceria solid solutions were made by a sol-gel method using the following salts: $Ce(NO_3)_3{\cdot}6H_2O$, $Gd(NO_3)_3{\cdot}xH_2O$ (x~6, Alfa Aesar, 99.9%), $Y(NO_3)_3{\cdot}6H_2O$ (Alfa Aesar, 99.9%), $La(NO_3)_3{\cdot}6H_2O$ (Alfa Aesar, 99.9%), $Sm(NO_3)_3{\cdot}6H_2O$ (Alfa Aesar, 99.9%), $Yb(NO_3)_3{\cdot}5H_2O$ (Aldrich Chem. Co., 99.999%), $Pr(NO_3)_3{\cdot}xH_2O$ (Alfa Aesar, 99.9%), $NbCl_5$ (Aldrich Chem. Co, 99%), $TaCl_5$ (Aldrich Chem. Co., 99.8%), and $ZrO(NO_3)_2{\cdot}xH_2O$ (Aldrich Chem. Co.). The salts were dissolved in distilled water and mixed to achieve the desired oxide concentration. The aqueous solutions were then dried at 373K and calcined at 873 K.

To determine whether the sol-gel methods used in the preparation of most of the samples could have resulted in segregation of the dopant to the surface, two samples were prepared using different synthesis conditions. First, a Sm-doped sample was prepared using the Pechini method. In this case, an aqueous solution of $Sm(NO_3)_3$ and $Ce(NO_3)_3$ was heated to 373 K, then citric acid was added to form the chelated ions. After the addition of ethylene glycol, the sample was heated at 413 K to form the solid precursor. Finally the precursor was calcined at 873 K. Second, a sample of Nb-doped ceria was synthesized using hydroxide co-precipitation. In this case, an aqueous solution of $Ce(NO_3)_3$ and $NbCl_5$ was precipitated using ammonium hydroxide, washed thoroughly with distilled water, dried at 373 K, and calcined in air at 873 K.

Sample Characterization

Phase identification was performed via x-ray diffraction with a Rigaku X-ray diffractometer using Ni-filtered Cu Kα radiation ($\lambda = 1.54060$ Å). The diffraction measurements were performed in the range of $2\theta = 20^\circ - 80^\circ$ with a scanning speed of 3° 2θ/min. Lattice parameters were calculated by using Bragg's law: $2d\sin\theta = n\lambda$. Calibration of the diffraction angles was obtained by mixing a small amount of NaCl with each of the samples.

The surface areas of all the samples were determined by measuring the quantity of iso-propanol adsorbed irreversibly at room temperature, using a Cahn 2000 microbalance, as described in other publication [33]. We assumed an adsorption stoichiometry of $6x10^{18}$ molecules/m^2 for calculating the surface areas. The microbalance was also used to examine CO_2 adsorption on the La-doped ceria samples to look for La_2O_3 segregation on the surface. These measurements rely on the fact that La_2O_3 forms a stable carbonate when exposed to CO_2 [34], while CeO_2, so long as it is completely oxidized, does not adsorb CO_2 [32]. After placing a sample onto the pan of the microbalance and heating it in vacuum to 723 K to remove adsorbed water, the powders were oxidized in 200 torr of O_2 at 723 K, evacuated, and then exposed to 200 torr of CO_2 at 723 K. After evacuating the sample once again, the quantity of CO_2 was measured by the mass change.

The n-butane oxidation rates were measured in a ¼-inch, Pyrex, tubular reactor operating at atmospheric pressure, using ~100 mg of sample. The flow rates of reactants were controlled with mass-flow controllers. Typical feed rates to the reactor were as follows: 2 ml/min n-butane, 16 ml/min O_2, and 102 ml/min of He. The reaction products were measured using a gas chromatograph (SRI8610C) equipped with a Hayesep Q column and a TCD detector. Before analysis of the products, most of the water was removed by a trap held in ice water. All rates were measured under differential conditions, with less than 10% conversion of the limiting reagent. Under the reaction conditions used in this study, the only products observed in significant quantities were CO_2 and water.

The reducibility of selected samples was also examined using CO. These samples were oxidized in pure O_2 at 673 K for 0.5 h. After being flushed in dry He at 873 K, they were then exposed to a flowing mixture of 4% CO in He at 873 K, while the CO consumption and CO_2 production were monitored using a quadrupole mass spectrometer. Finally, residual CO_2 adsorbed on reduced ceria was removed from the samples by exposure to O_2, although the amount of CO_2 produced in this final step was never more than 5% of the total CO_2 that was formed on the sample.

X-ray photoelectron spectroscopy (XPS) experiments were conducted in an ultra-high vacuum chamber (base pressure of 2×10^{-10} Torr) equipped with a hemispherical electron energy analyzer and x-ray source. Calcined powders were pressed and then examined without additional pretreatment.

Results

The physical characteristics of selected samples are given in Table 1. The surface areas were found to be in the range between 7 and 25 m^2/g. All of the doped samples had lower surface areas than that was found for pure ceria; however, the differences observed for the surface areas are small compared to the differences that were found in the reaction rates to be discussed shortly. Lattice parameters for each sample are also reported in Table 1. In all cases, only a single, cubic phase was observed in x-ray diffraction. Furthermore, with the exception of the Nb sample, changes in the lattice parameter of the cubic phase indicated that solid solutions had been formed. For the +3 ions, lattice parameters for the solid solutions have been reported and our observed lattice parameters are in good agreement with literature values for those cases [23, 35]. For Nb-doped ceria, the fact that there is no change in the lattice parameter may indicate that the Nb does not substitute for Ce atoms in the fluorite structure.

Fig.1 shows the reaction rates, measured under differential conditions with 12 torr of n-butane and 100 torr of O_2, for selected samples from Table 1. Table 2 summarizes the rate data for all the samples from Table 1. Because the amount of catalyst in the reactor was approximately constant for each of the samples, rates on the most active samples were measured at lower temperatures. Also, it was necessary to extrapolate some of the measured rates in Table 2 in order to compare all of the samples under similar conditions. Clearly, the most catalytically active samples were the pure ceria and the $Zr_{0.2}Ce_{0.8}O_2$ samples. The reaction rate on pure ceria also exhibited the highest activation energy, 125 ± 5 kJ/mol.

Comparing first the $Zr_{0.2}Ce_{0.8}O_2$ and CeO_2 samples, our results show a minimal difference in the reactivity of these two catalysts. From the literature, it is well known that ceria-zirconias exhibit superior catalytic properties compared to pure ceria. However, the superiority of ceria-zirconias is primarily because the mixed oxide is more stable to high-temperature treatments [12,13]. Also, the concentration of Zr in most catalyst applications is considerably higher than we have used here.

It is informative to consider the ceria samples doped with +3 ions next. All of these samples are much less active than pure ceria, with Yb-doped ceria being 100 times less active and Sm-doped ceria being 500 times less active at 650 K. The large differences in the reaction rates observed on the doped-ceria samples cannot be explained by the small differences in surface area observed on the doped samples. Also, if Sm_2O_3 were to segregate to the surface of ceria and simply block sites, the samaria layer would need to cover the ceria in an extremely even manner to explain such a large decrease in rates. Further evidence that surface segregation of samaria cannot simply explain the lower rates on Sm-doped ceria comes from the fact that rates on the sample prepared by the Pechini method showed almost identical rates to the sample prepared by sol-gel methods. Because the Pechini method involves the addition of a chelating agent to maintain mixing on the atomic scale before calcination, one should expect that this sample would be a solid solution, or at least very different from the sample prepared by sol-gel methods.

A second interesting point regarding the data on the ceria samples doped with +3 ions is the fact that strongest effects are observed with those ions that are the best dopants for enhancing the ionic conductivity of ceria. The lowest rates are observed with Sm and Gd doping and these ions are known to provide the highest ionic conductivity in doped ceria [23]. The explanation for the effectiveness of these two ions in promoting ionic conductivity is likely that these ions have the optimal size for allowing oxygen-ion mobility [24]. Finally, it is noteworthy that the relative activity of the doped samples correlates with their activation energies, with the most active samples exhibiting the highest activation energies.

The results for Nb, Ta, and Pr doping should be considered separately. Since x-ray diffraction failed to show a change in the lattice parameter with Nb doping, it is unclear that one should view this or the Ta-doped sample as being a solid solution, even though we did not detect a separate Nb_2O_5 phase; however, solutions of Nb_2O_5 and ZrO_2 are known [36], so that solutions with CeO_2 are possible and likely. Again, given the fact that the rates on the Nb and Ta-doped ceria were more than 500 times lower than that of pure ceria, any niobia or tantala surface layer would need to be extremely effective in blocking the surface of ceria. With Pr doping, the lattice parameter change would suggest that a solid solution had been formed. While the rates on this sample were not as severely attenuated as on the other doped ceria, they were still 28 times lower than that observed on pure ceria.

Fig. 2 shows the results of an investigation on the effect of dopant levels for Sm and Gd on the rate of n-butane oxidation in 12 torr n-butane and 100 torr O_2, with the data for Sm-doped ceria in Fig. 2a) and the data for Gd-doped ceria in Fig. 2b). Clearly, the reaction rates decrease progressively with increasing dopant concentration, consistent with the findings in Fig. 1. However, the activation energies for the doped samples were similar, independent of dopant level. It appears that additional amounts of Sm or Gd dopants primarily change the number of active sites, although that would imply all of the sites present on pure ceria have been removed by the addition of even small quantities of dopant and substituted with a new type of less reactive site.

The rates in Fig. 1 and Table 1 were obtained with a stoichiometric O_2:n-butane ratio. To determine whether the differences observed in the reactivity for ceria and Sm-doped ceria apply to various n-butane:O_2 stoichiometries, rates were measured at the stoichiometries shown in Table 3, holding the total flow rate 120ml/min. While we did not carry out a careful determination of activation energies at these other stoichiometries, it was necessary to carry out the reaction at a significantly higher temperature on the Sm-doped ceria, 673 K compared to 533 K, in order to obtain comparable rates.

For ceria, it is possible to determine when the sample is partially reduced by visual inspection. Ceria is a light yellow in color when it is completely oxidized, but turns dark when it is even partially reduced due to electronic conductivity associated with Ce^{+3}. For all of the samples and all of the n-butane:O_2 stoichiometries investigated in this study, the ceria was completely oxidized. This was demonstrated by switching the gas composition in the reactor from the n-butane-O_2-He mixture to pure He, then cooling the sample to room temperature and simply looking at the catalyst. Since the oxidation of n-butane must involve a redox mechanism in which ceria is reduced by n-butane, then reoxidized by O_2, the fact that the samples remained oxidized, even in excess n-butane, implies that the reoxidation reaction must be much faster than the rate of ceria reduction by n-butane. Obviously, one would expect this conclusion to change when the reaction is carried out in excess n-butane at higher conversions, since the catalyst would then see a much higher n-butane:O_2 ratio.

To determine whether the doped-ceria samples were indeed reducible, we examined the amount of oxygen that could be removed from selected samples upon heating in 4% CO-He mixture at 873 K, with results shown in Table 4. Because Ce_2O_3 and many of the dopants can form stable carbonates, which would greatly complicate the interpretation of reaction temperatures, we did not attempt to measure the temperature at which reduction begins on these samples. For pure ceria, the total amount of oxygen atoms that could be removed was 1.33 mmol/g, a number that is significantly less than 2.9 mmol/g, the quantity that would be expected for complete reduction of CeO_2 to Ce_2O_3. The quantity of oxygen that could be removed from the doped samples was less than that which could be removed from pure CeO_2 and decreased with the reactivity of the doped samples, with $Yb_{0.2}Ce_{0.8}O_{1.9} > Y_{0.2}Ce_{0.8}O_{1.9} > La_{0.2}Ce_{0.8}O_{1.9} > Gd_{0.2}Ce_{0.8}O_{1.9} > Sm_{0.2}Ce_{0.8}O_{1.9}$. Substitution of a +3 ion in place of Ce^{+4} should decrease the reducibility of the sample; but it is unclear whether the change in the amount of oxygen that can be removed is related to the steady-state reactivity changes, even though the trends clearly are the same.

Finally, we performed two tests to look for surface segregation in La-doped ceria to determine whether this could be the cause for decreased reaction rates. In Fig. 3, XPS results are shown for a sample prepared by physically mixing pure CeO_2 and La_2O_3 powders in a ratio of 4:1 and for the $La_{0.2}Ce_{0.8}O_{1.9}$ sample. The La(3d) peaks are clearly more intense for $La_{0.2}Ce_{0.8}O_{1.9}$, which would suggest there might be surface enrichment of La relative to Ce. However, since the escape depth of electrons at these energies is greater than 1 nm, one cannot determine from XPS whether the additional La atoms are at the surface or simply near the surface.

To examine the surface composition, we measured CO_2 adsorption on oxidized samples of CeO_2, $La_{0.2}Ce_{0.8}O_{1.9}$, and La_2O_3 at room temperature. For oxidized CeO_2, the CO_2 uptake was less than 0.05 mg/g, while the uptakes on $La_{0.2}Ce_{0.8}O_{1.9}$ and La_2O_3 were 0.84 mg/g and 6.5 mg/g respectively. Earlier studies on reduced ceria indicated that a carbonate monolayer should contain $\sim 6 \times 10^{18}$ CO_2 molecules/m^2 [32], a value that is close to the coverage expected for a close-packed layer of molecules the size of the carbonate anion. Based on that specific coverage, the pure La_2O_3 sample would have a surface area of 15 m^2/g, a value that is similar to the surface areas obtained on the other samples in this study. By comparison, the CO_2 uptake on $La_{0.2}Ce_{0.8}O_{1.9}$ corresponded to 6×10^{17} molecules/m^2. Assuming that surface layers of lanthana on ceria would have similar chemical properties to bulk lanthana, the $La_{0.2}Ce_{0.8}O_{1.9}$ sample cannot simply be coated by a chemically inert layer of lanthana.

Discussion

It is rather surprising that the addition of many dopants to ceria decreases the activity of ceria for n-butane oxidation. The decreases are so large that it seems unlikely that ceria could simply be covered by the second oxide. For rates to decrease by a factor of more than 100, the catalytic sites on the surface would need to blocked very effectively. Therefore, the decrease in reaction rates raises a large number of questions.

First, we cannot rule out that there will be some segregation of the dopants to the surface, even though the XRD results for most of the samples are consistent with single-phase, solid solutions. In addition to the XPS results shown here, there are some indications that enrichment should be expected for at least some of these dopants. For example, energy-minimization calculations of CeO_2 reduction indicate that Ce^{+3} ions should form most easily at the surface because this will minimize the penalty associated with the lower Coulombic attraction of +3 ions with lattice-oxygen anions [37]. There are also indications from Low Energy Ion Scattering studies with $Gd_{0.2}Ce_{0.8}O_{1.9}$ that the surface is enriched to a Ce:Gd ratio of 1 [38]. Even if one assumes the surface composition is similar to the bulk concentration, it is reasonable that the presence of dopant atoms in the surface could affect the reactivity of the remaining ceria, perhaps by decreasing the reducibility of the remaining Ce^{+4} or by decreasing the ability of Ce cations to stabilize alkyl fragments that must be part of the reaction mechanism.

Second, one cannot assume that the doped-ceria catalysts will show lower activities for all reactions or that the activity will be independent of the oxidation state of the catalyst. Certainly, there have been temperature-programmed-reduction (TPR) studies that have shown that some doped cerias reduce at a lower temperature than pure ceria [26,39]. This in turn would imply that doped ceria can indeed exhibit higher rates than ceria for H_2 oxidation in the absence of O_2. However, TPR results may not be relevant for reactions other than H_2 oxidation and the oxidation state of the catalyst may be very different in TPR and steady-state-reaction conditions. In our studies, the samples were always in a completely oxidized state, while the oxidation state of cerium is clearly changing during the course of a TPR measurement. Furthermore, since reoxidation of the catalyst is fast in n-butane oxidation (as demonstrated by the fact that ceria was always completely oxidized in our studies), the rate-limiting step in n-butane oxidation likely involves breaking of a C-H or C-C bond, assisted by the surface. The ability of the catalyst to assist in bond breaking may or may not be related to the reducibility of the sample. The implication of this is that doping may affect the rates of various reactions in different ways.

In comparing the effect of dopants with a +3 charge, it is very interesting that rates were decreased most by those elements that most increase ionic conductivity, namely Sm^{+3} and Gd^{+3}. The activation energy for reaction was also affected most strongly by these elements. It is not clear why catalytic properties and ionic-conductivities should be related. One explanation for this might be that Ce^{+3} ions on the surface are necessary for stabilization of alkyl fragments and that high ionic conductivity enhances the reoxidation rate by lattice oxygen. Another possible explanation is that the same lattice distortions, caused by the dopant, that lead to high ionic conductivity in the bulk lead to a lower reactivity of sites on the surface.

The fact that n-butane oxidation rates on CeO_2 are suppressed by doping with Ta^{+5} and Nb^{+5} to a similar extent as with other oxides would be consistent with the idea that surface composition is crucial, since one would not expect Nb and Ta to affect the bulk properties of ceria in the same way as the +3 ions. If Nb^{+5} and Ta^{+5} share sites with Ce^{+4} on the surface, it may that the presence of a second type of cation on the surface, either +3 or +5 cations, destabilizes a critical intermediate in the reaction. While the suppression of reaction rates is less severe with the addition of Pr, it may well be that Pr has some activity on its own. It has been suggested elsewhere that PrOx is relatively inactive compared to ceria due to the high stability of Pr_2O_3 [27].

The suppression of rates on ceria by the addition of a second oxide is reminiscent of the deactivation that is observed following high-temperature treatment of ceria [11], although we believe the mechanism for deactivation by dopants is likely very different. Indeed, we have found that Pd supported on Sm-doped ceria exhibits similar rates for the water-gas-shift reaction as normal Pd-ceria catalysts [40], while a Pd catalyst supported on ceria that has been calcined to high temperatures is inactive [41].

Perhaps the most important point to be made about the results in this paper is that one should not assume that additives which promote one property (i.e. ionic conductivity) will promote another (i.e. catalytic activity). Furthermore, with mixed oxides, the addition of relatively small quantities of a second oxide can dramatically affect catalysis on the primary component. Clearly, there is much we want to learn about these materials and how best to use them.

Conclusions

Doping CeO_2 withYb_2O_3, Y_2O_3, Sm_2O_3, Gd_2O_3, La_2O_3, Nb_2O_5, Ta_2O_5, or Pr_6O_{11} has a strong and deleterious effect on the catalytic activity of ceria for n-butane oxidation. The common assumption that doping of CeO_2 will lead to higher reaction rates should always be tested for the targeted reaction.

Acknowledgements

This work was supported by the DOE, Basic Energy Sciences, Grant #DE-FG03-85-13350.

References

1) M. Primet and E. Garbowski, in: A. Trovarelli, (Ed.), Catalysis by Ceria and Related Materials, Imperial College Press, London, 2002, p. 407-429.
2) Alessandro Trovalelli, Carla de Leitenburg, Marta Boaro, Giuliano Dolcetti, Catal. Today 50 (1999) 353.
3) T. Hattori, J. Inoko, Y. Murukami, J. Catal., 42 (1976) 60.
4) S. McIntosh, J. M. Vohs, R. J. Gorte, Electrochim. Acata, 47 (1002) 3815.

5) R. J. Farrauto, C. H. Bartholomew, in: Fundamentals of Industrial Catalytic Processes", Blackie Academic & Professional, London, 1997, p. 606.
6) R. J. Farrauto, K. E. Voss, and R. M. Heck, US Patent #5,462,907 (1995).
7) G. S. Zafiris and R.J. Gorte, J. Catal. 139 (1993) 561.
8) G. S. Zafiris, R.J. Gorte, J. Catal. 143 (1) (1993) 86.
9) T. Bunluesin, H. Cordatos, R.J. Gorte, J. Catal. 157 (1995) 222.
10) M. Y. Smirnov, G.W. Graham, Catal. Lett. 72 (2001) 39.
11) H. Cordatos, T. Bunluesin, J. Stubenrauch, J.M. Vohs, and R.J. Gorte, J. Phys. Chem. 100 (1996) 785.
12) T. Bunluesin, R.J. Gorte, G.W. Graham, Appl. Catal. B 14 (1997) 105.
13) T. Bunluesin, R.J. Gorte, G.W. Graham, Appl. Catal. B 15 (1998) 107.
14) R. M. Ferrizz, G.S. Wong, T. Egami, J.M. Vohs, Langmuir 17 (2001) 2464.
15) S. H. Overbury, D.R. Mullins, D.R. Huntley, L. Kundakovic, J. Phys. Chem. B 103 (1999) 11308.
16) M. Shelef, G. W.Graham and R.W. McCabe, in: A. Trovarelli, (Ed.), Catalysis by Ceria and Related Materials, Imperial College Press, London, 2002, p. 343-376.
17) X. Wang, R. J. Gorte, and J. Wagner, J. Catal. 212 (2002) 225.
18) J. Kaspar and P. Fornasiero, in: A. Trovarelli, (Ed.), Catalysis by Ceria and Related Materials, Imperial College Press, London, 2002, p. 217-241.
19) T. Egami, W. Dmowski, R. Brezny, SAE J. 1997 Paper No. 970461.
20) E. S. Putna, J.M. Vohs, R.J. Gorte, Catal. Lett. 45 (1997) 143.
21) R. M. Ferrizz, T. Egami, J.M. Vohs, Surf. Sci. 465 (2000) 127.
22) E. Mamontov and T. Egami, J. Phys. Chem. B 104 (2000) 11110.
23) K. Eguchi, T. Setoguchi, T. Inoue, and H. Arai, Solid State Ionics, 52 (1992) 165.
24) H. Hayashi, R. Sagawa, H. Inaba, and K. Kawamura, Solid State Ionics, 131 (2000) 281.
25) M. O'Connell and M. A. Morris, Catal. Today, 59 (2000) 387.
26) E. Ramirez-Cabrera, A. Atkinson, and D. Chadwick, Appl. Catal. B, 36 (2002) 193.
27) E. S. Putna, J.M. Vohs, R.J. Gorte, G.W. Graham, Catal. Lett. 54 (1998) 17.
28) C. K. Narula, K.L. Taylor, L.P. Haack, L.F. Allard, A. Datye, M.Y. Slnev, M. Shelef, R.W. McCabe, W. Chun, G.W. Graham Mater. Res. Soc. Symp. Proc. 497 (1998) 15-20.
29) S. Park, J. M. Vohs, and R. J. Gorte, Nature, 404 (2000) 265.

30) R.J. Gorte, S. Park, J.M. Vohs, C. Wang, Adv. Mater. 12 (2000) 1465.
31) X. Wang, R.J. Gorte, Appl. Catal. A 224 (2002) 209.
32) S. Sharma, S. Hilaire, J.M. Vohs, R.J. Gorte, H-W. Jen, J. Catal. 190(2000) 199.
33) A.I. Biaglow, R.J. Gorte, S. Srinivasan, A.K. Datye, Catal. Lett. 13 (1992) 313.
34) E. S. Putna, B. Shereck, R.J. Gorte, Appl. Catal. B, 17 (1998) 101-106.
35) J. Li, T. Ikegami, T. Mori, and T. Wada, Chem. Mater. 13 (2001) 2913.
36) J.G. Thompson, R.L. Withers, J. Sellar, P.J. Barlow, B.G. Hyde, J. Solid State Chem. 88 (1990) 465.
37) H. Cordatos, D. Ford, R.J. Gorte, J. Phys. Chem. 100 (1996) 18128.
38) J.G. Thompson, R.L. Withers, J. Sellar, P.J. Barlow, B.G. Hyde, J. Solid State Chem. 88 (1990) 465.
39) P. J. Scanlon, R.A.M. Bink, F.P.F. van Berkel, G.M. Christie, L.J. van Ijzendoorn, H.H. Brongersma, R.G. van Welzenis, Solid State Ionics, 112 (1998) 123.
40) X. Wang and R. J. Gorte, Appl. Catal. A, in press.
41) W. Shen, Y. Ichihashi, H. Ando, Y. Matsumura, M. Okumura, M. Haruta, Appl. Catal. A 217 (2001) 231.

Table 1: The surface areas and lattice parameters of samples used in this study.

Catalyst	Surface area m^2/g	Lattice Parameter ± 0.001 nm
CeO_2	25	0.540
$Yb_{0.2}Ce_{0.8}O_{1.9}$	14	0.539
$Y_{0.2}Ce_{0.8}O_{1.9}$	10	0.541
$La_{0.2}Ce_{0.8}O_{1.9}$	15	0.547
$Gd_{0.2}Ce_{0.8}O_{1.9}$	7	0.542
$Sm_{0.2}Ce_{0.8}O_{1.9}$	18	0.544
$Sm_{0.2}Ce_{0.8}O_{1.9}$ (Pechini method)	11	0.544
$Nb_{0.1}Ce_{0.9}O_{2.05}$	18	0.540
$Nb_{0.1}Ce_{0.9}O_{2.05}$ (Coprecipitation)	18	0.539
$Ta_{0.1}Ce_{0.9}O_{2.05}$	23	0.538
$Pr_{0.2}Ce_{0.8}O_{2.05}$	14	0.542

Table 2: Differential rates and activation energies for n-butane oxidation.

Catalyst	Rate at 650 K (molecules/s·g)[a]	Rate at 650K (molecules/$s\cdot m^2$)	Activation Energy ± 5 (kJ/mol)[b]
CeO_2	5.1 x 10^{19} [c]	2.0 x 10^{18}	125
$Zr_{0.2}Ce_{0.8}O_{1.9}$	2.4 x 10^{19} [c]	-----	115
$Yb_{0.2}Ce_{0.8}O_{1.9}$	4.2 x 10^{17}	3.0 x 10^{16}	105
$Y_{0.2}Ce_{0.8}O_{1.9}$	3.8 x 10^{17}	3.8 x 10^{16}	60
$La_{0.2}Ce_{0.8}O_{1.9}$	1.6 x 10^{17}	1.1 x 10^{16}	80
$Gd_{0.2}Ce_{0.8}O_{1.9}$	1.2 x 10^{17}	1.7 x 10^{16}	65
$Sm_{0.2}Ce_{0.8}O_{1.9}$	1.0x 10^{17}	5.5 x 10^{15}	70
$Sm_{0.2}Ce_{0.8}O_{1.9}$ (Pechini method)	1.4 x 10^{17}	1.3 x 10^{16}	105
$Nb_{0.1}Ce_{0.9}O_{2.05}$	1.1 x 10^{17}	6.1 x 10^{15}	105
$Nb_{0.1}Ce_{0.9}O_{2.05}$ (Coprecipitation)	1.4 x 10^{17}	6.4 x 10^{15}	85
$Ta_{0.1}Ce_{0.9}O_{2.05}$	1.1 x 10^{17}	4.8 x 10^{15}	115
$Pr_{0.2}Ce_{0.8}O_{2.05}$	1.8 x 10^{18} [c]	1.3 x 10^{17}	120

a) The data are calculated using Arrhenius equation.
b) The activation energy is from Arrhenius plots.
c) The data are extrapolated from the Arrhenius plots. Rate of CeO_2 is extrapolated from 533K, while rates of $Yb_{0.2}Ce_{0.8}O_{1.9}$ and $Pr_{0.2}Ce_{0.8}O_{2.05}$ are extrapolated from 593K.

Table 3: n-Butane reaction rates at various n-butane:O_2 ratios.

	CeO_2 at 533K	$Sm_{0.2}Ce_{0.8}O_{1.9}$ at 673K
Butane:O_2 = 2.75:1	1.2 x 10^{18}	4.8 x 10^{17}
Butane:O_2 = 1:1.5	3.1 x 10^{17}	1.0 x 10^{17}
Butane:O_2 = 1:8	3.1 x 10^{17}	1.8 x 10^{17}
Butane:O_2 = 1:13	3.8 x 10^{17}	2.5 x 10^{17}
Butane:O_2 = 1:32.5	9.3 x 10^{17}	4.0 x 10^{17}

Table 4: Oxygen removed by CO consumption at 873K.

Catalyst	CO consumption µmol/g
CeO_2	1330
$Yb_{0.2}Ce_{0.8}O_{1.9}$	1240
$Y_{0.2}Ce_{0.8}O_{1.9}$	1170
$La_{0.2}Ce_{0.8}O_{1.9}$	1110
$Gd_{0.2}Ce_{0.8}O_{1.9}$	870
$Sm_{0.2}Ce_{0.8}O_{1.9}$	760

Figure Captions:

Fig.1. Differential reaction rates for n-butane oxidation on doped cerias. The symbols correspond to the following catalysts: ▲ CeO_2; ◊ $Zr_{0.2}Ce_{0.8}O_{2}$; ● $Yb_{0.2}Ce_{0.8}O_{1.9}$; ○ $Pr_{0.2}Ce_{0.8}O_{2}$; ◆$La_{0.2}Ce_{0.8}O_{1.9}$; □ $Sm_{0.2}Ce_{0.8}O_{1.9}$; Δ $Nb_{0.1}Ce_{0.9}O_{2.05}$;.

Fig.2 (a): The effect of dopant levels for Sm_2O_3 in CeO_2. The catalyst compositions are as follows: CeO_2 (●); $Sm_{0.05}Ce_{0.95}O_{1.975}$ (◊); $Sm_{0.1}Ce_{0.9}O_{1.95}$ (◆); $Sm_{0.2}Ce_{0.8}O_{1.9}$ (□).

Fig.2 (b): The effect of dopant levels for Gd_2O_3 in CeO_2. The catalyst compositions are as follows: CeO_2 (▲); $Gd_{0.05}Ce_{0.95}O_{1.975}$ (○); $Gd_{0.1}Ce_{0.9}O_{1.95}$ (◆); $Gd_{0.2}Ce_{0.8}O_{1.9}$ (Δ).

Fig. 3: XPS spectra two La_2O_3-CeO_2 samples having a Ce:La ratio of 4. The top spectrum was from a mixed powder and bottom spectrum from the solid solution.

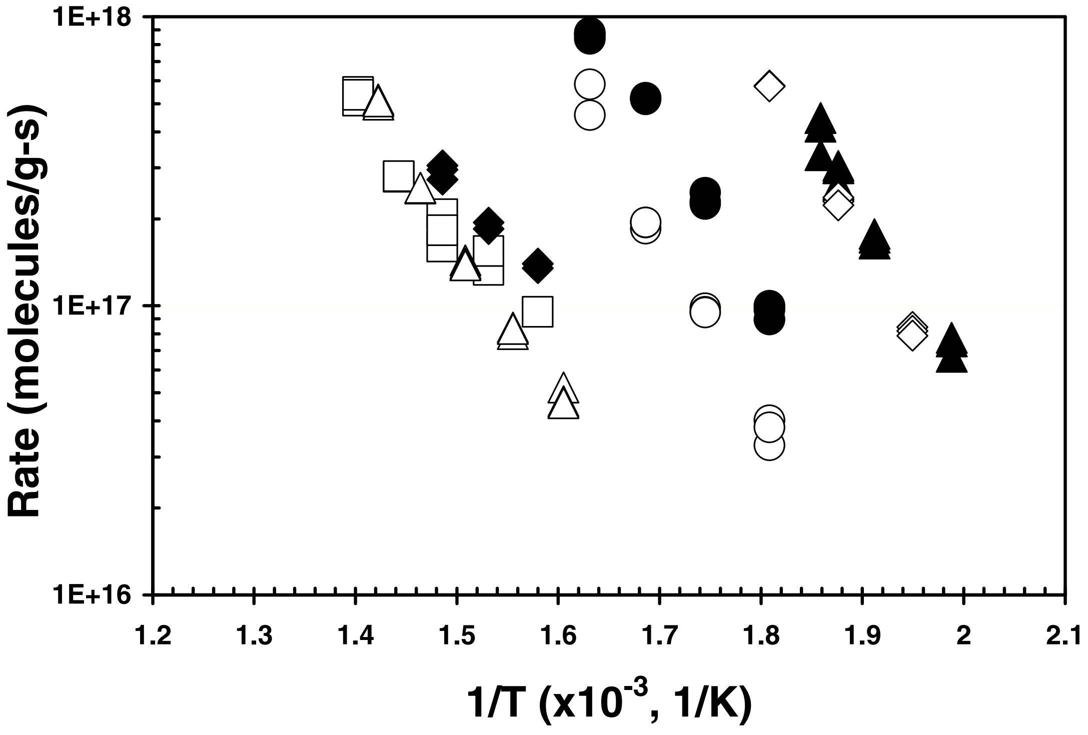

1E+18
1E+17
1E+16
Rate (molecules/g-s)
1.2
1.3
1.4
1.5
1.6
1.7
1.8
1.9
2
2.1
1/T (x10^-3, 1/K)

Fig. 1

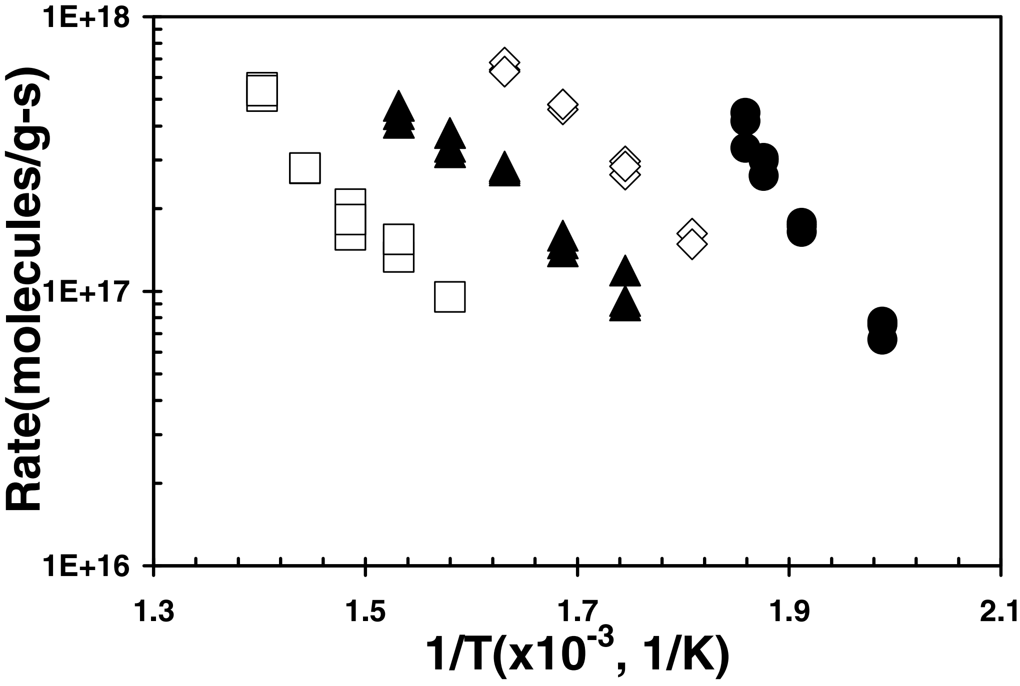

Fig. 2a)

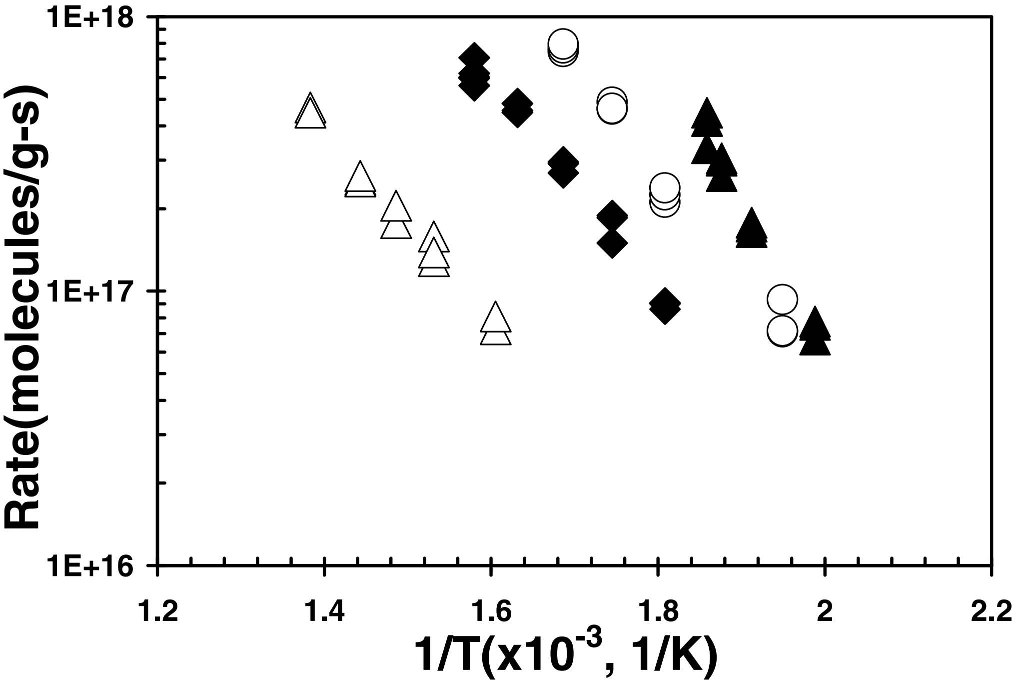

Fig. 2b)

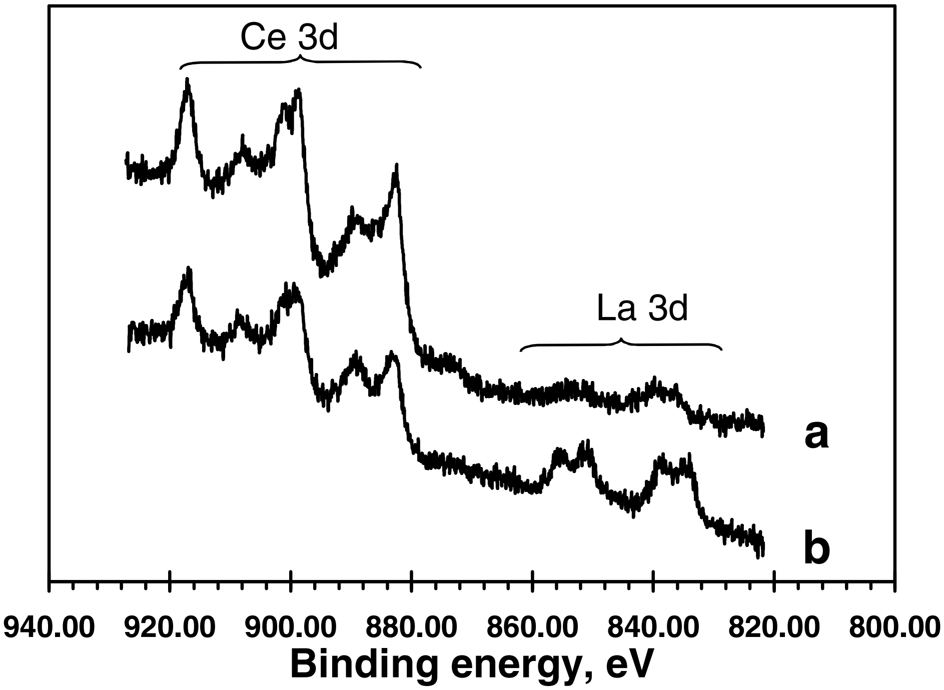
Ce 3d
La 3d
a
b
940.00
920.00
900.00
880.00
860.00
840.00
820.00
800.00
Binding energy, eV

Fig. 3.